



1 Distribution of Water Masses in the Atlantic Ocean based on 2 GLODAPv2

3 Mian Liu¹, Toste Tanhua¹

4 ¹GEOMAR Helmholtz Centre for Ocean Research Kiel, Marine Biogeochemistry, Chemical Oceanography, Düsterbrooker
5 Weg 20, 24105 Kiel, Germany

6 *Correspondence to:* T. Tanhua (ttanhua@geomar.de)

7



8 **Abstract:** The distribution of the main water masses in the Atlantic Ocean are investigated with the Optimal Multi-
 9 Parameter (OMP) method. The properties of the main water masses in the Atlantic Ocean are described in a companion
 10 article; here these definitions are used to map out the general distribution of those water masses. Six key properties,
 11 including conservative (potential temperature and salinity) and non-conservative (oxygen, silicate, phosphate and nitrate),
 12 are incorporated into the OMP analysis to determine the contribution of the water masses in the Atlantic Ocean based on the
 13 GLODAP v2 observational data. To facilitate the analysis the Atlantic Ocean is divided into four vertical layers based on
 14 potential density. Due to the high seasonal variability in the mixed layer, this layer is excluded from the analysis. Central
 15 waters are the main water masses in the upper/central layer, generally featuring high potential temperature and salinity and
 16 low nutrient concentrations and are easily distinguished from the intermediate water masses. In the intermediate layer, the
 17 Antarctic Intermediate Water (AAIW) from the south can be detected to $\sim 30^\circ\text{N}$, whereas the Subarctic Intermediate Water
 18 (SAIW), having similarly low salinity to the AAIW flows from the north. Mediterranean Overflow Water (MOW) flows
 19 from the Strait of Gibraltar as a high salinity water. NADW dominates the deep and overflow layer both in the North and
 20 South Atlantic. In the bottom layer, AABW is the only natural water mass with high silicate signature spreading from the
 21 Antarctic to the North Atlantic. Due to the change of water mass properties, in this work we renamed to North East Antarctic
 22 Bottom Water NEABW north of the equator. Similarly, the distributions of Labrador Sea Water (LSW), Iceland Scotland
 23 Overflow Water (ISOW), and Denmark Strait Overflow Water (DSOW) forms upper and lower portion of NADW,
 24 respectively roughly south of the Grand Banks between ~ 50 and 66°N . In the far south the distributions of Circumpolar
 25 Deep Water (CDW) and Weddell Sea Bottom Water (WSBW) are of significance to understand the formation of the AABW.

26
 27 **Key words:** Water Masses, Optimal-Multi-Parameter Analysis, Atlantic Ocean

28

29



1. Introduction

The distribution of properties in the ocean tends to be distributed along bodies of water with similar history, or water masses (Mackas et al., 1987). The properties of water masses further more tend to change along the flow path of a water mass, partly due to biological or chemical changes, i.e. non-conservative behavior of properties, and due to mixing with surrounding water masses (Hinrichsen and Tomczak, 1993; Klein and Tomczak, 1994). Knowledge of the distribution and variation of water masses is of fundamental importance in oceanography, particularly for biogeochemical and biological applications where the transformation of properties over time can be successfully viewed in the water mass frame-work. For instance, the process of deep water formation from near surface waters enable the effects of air-sea gas exchange to penetrate the deep waters. In the North Atlantic deep water formation transports anthropogenic carbon and oxygen from the surface to the deep ocean (e.g. Garcia-Ibanez et al., 2015). Furthermore, the interactions of water masses influence the distribution of biologically important elements, such as oxygen, carbon and nutrients (e.g. Karstensen et al., 2008). All of these studies show that the study of water masses plays not only an important role in physical oceanography, but also irreplaceable role in biogeochemistry.

With an increasing number of publications focusing on water mass characterization on a global (e.g. Stramma and England, 1999) and regional scale (e.g. Carracedo et al., 2016; Talley, 1996), differences in research goals and areas has resulted in different definitions and names of water masses by researchers. For example, in a study focusing on T-S distribution, shallow water masses are named as Mode Water due to their linear, T-S relationship (McCartney and Talley, 1982). But other works referred the same water masses as Central Water, since the authors focused more on the distribution and transport of mass and chemical constituents (Garcia-Ibanez et al., 2015). Here we follow the approach by Garcia-Ibanez et al. (2015) and utilize the definitions of water masses that we present in a companion paper to map out the general distribution of water masses in the Atlantic Ocean.

In the Atlantic Ocean, warm upper/central waters are generally transported northward into the high latitude North Atlantic, where the dense and cold deep water is formed, and subsequently sinks and spreads southward across the equator into the South Atlantic (Fyfe et al., 2007).

Consistent with the work in our companion paper (Liu and Tanhua, 2019), we divide the water column into four vertical layers based on potential density (σ_θ). Water masses in the upper/central layer ($\sigma_\theta < 27 \text{ kg/m}^3$) origin from seawater that subduct into the thermocline during winter time. Four water masses are located in this layer: the East North Atlantic Central Water (ENACW), West North Atlantic Central Water (WNACW), East South Atlantic Central Water (ESACW) and West South Atlantic Central Water (WSACW). In the intermediate layer ($\sigma_\theta = 27 - 27.7 \text{ kg/m}^3$), three water masses are identified. In the South Atlantic, Antarctic Intermediate Water (AAIW) originates from the surface (upper 200m) in the region north of Antarctic Circumpolar Current (ACC) and east of Drake Passage (Alvarez et al., 2014; Talley, 1996). In the North Atlantic,



Subarctic Intermediate Water (SAIW) originates from surface in the western boundary of Subpolar Gyre and spreads southward along the Labrador Current (Pickart et al., 1997). In the east, Mediterranean Overflow Water (MOW) flows through the Strait of Gibraltar with a feature of high salinity. North Atlantic Deep Water (NADW) is the dominant water mass in the deep and overflow layer ($\sigma_\theta = 27.7 - 27.88 \text{ kg/m}^3$). This water mass is formed in the high latitude North Atlantic, with relatively high potential density due to the low potential temperature and high salinity. We further divide the NADW into upper and lower portions by different potential density and origins. Labrador Sea Water (LSW) is the origin of upper version of NADW (uNADW) whereas Iceland-Scotland Overflow Water (ISOW) and Denmark Strait Overflow Water (DSOW) are origins of lower NADW. Antarctic Bottom Water (AABW) is the main water mass in the bottom layer ($\sigma_\theta > 27.88 \text{ kg/m}^3$). This water mass is a mixed product between Weddell Sea Bottom Water (WSBW) and Circumpolar Deep Water (CDW) (van Heuven et al., 2011; Weiss et al., 1979). In regions north of the equator we define AABW as a new water mass, the Northeast Atlantic Bottom Water (NEABW).

2. Data and Methods

There are some key features of the distribution of properties that are well known, but never the less are helpful in understanding the distribution of water masses in the Atlantic Ocean. We use a meridional section across the Atlantic Ocean to illustrate this, the WOCE/GO-SHIP A16 section as occupied by cruise 33RO20130803 (North Atlantic) & 33RO20131223 (South Atlantic), Figure 1. In the upper layer, high temperatures, salinities and low nutrients, especially nitrate can be seen on the section plots. The above characteristics are consistent with the properties of central water masses. The intermediate layer is characterized by low salinity and high nitrate and silicate in the South Atlantic. According to this feature, the location of AAIW can be initially determined. And relative high salinity distributes around 40°N is the signal of MOW. High oxygen in the north helps to label SAIW. Relative higher salinity and oxygen but lower nutrients (silicate and nitrate) are important signals of water masses in deep and overflow layer (upper and lower NADW) to distinguish from intermediate and bottom waters. High silicate is one significant property to identify AABW in bottom layer. Also this layer has the lowest potential temperature. In the north hemisphere, there is a sudden reduction of silicate compared with south of equator. This is the reason that a new water mass, NEABW, is defined in this region.

2.1. The GLODAPv2 dataset

Marine surveys from different countries are actively organized and coordinated since late 1950s, after the establishment of the Scientific Committee for Marine Research (SCOR) in 1957 and the Intergovernmental Oceanographic Commission (IOC) in 1960. And meanwhile, academic exchanges between world countries and organizations became frequent and popular. WOCE (the World Ocean Circulation Experiment), JGOFS (Joint Global Ocean Flux Study) and OACES (Ocean Atmosphere Carbon Exchange Study) are the three most typical representatives after entering 1990s. However, these programs are initiated by different countries and with their respective aims and goals. Hence, coordination and collaboration between the countries are necessary and beneficial. GLODAP (Global Ocean Data Analysis Project) is a data product that



came into being in this context. In addition to create a global dataset based on above programs, the goals of GLODAP include also to describe distribution and biogeochemical properties in the global ocean and to make data publicly available (Key et al., 2004). The GLODAP dataset shows a good start for global data sharing however the shortcomings also cannot be ignored. From the spatial scale, few data in high latitude region, north of 60 °N or in the Arctic region, are collected in this dataset, and meanwhile, data from Mediterranean Sea are also not included. In the term of time, GLODAPv1.1 contains data only until 1999. The updated and expanded dataset GLODAPv2 successfully made up for the above disadvantages (Lauvset et al., 2016). In addition to the integration of two other datasets, CARINA (CARbon dioxide IN the Atlantic Ocean, Key et al., 2010) and PACIFICA (PACIFIC ocean Interior Carbon, Ishii et al., 2011), GLODAPv2 also includes an 168 additional independent cruises those never been collected by any datasets. Thus GLODAPv2 is a dataset that includes relatively complete data and with an almost global coverage, and also include a mapped product.

2.2. OMP Analysis

For the water mass analysis we used in total 6 key properties, including two conservative (potential temperature and salinity) and four non-conservative (oxygen, silicate, phosphate and nitrate) properties to define the Source Water Types (SWTs) as origins of water masses, see the companion study (Liu and Tanhua 2019 for details). Based on the above observational data, it is obviously not enough to make accurate estimation of the distribution of the water masses only by displaying key properties. In order to determine the distribution of water masses exactly, we have to resort to more accurate mathematical calculations. Since the first publication of global distributions of water masses (Sverdrup, 1942), early studies on water masses are mainly based on potential temperature and salinity. Emery and Meincke made on summary and review on this kind of analysis in 1986 (Emery and Meincke, 1986). The limitation of this method is that distribution of more (more than three) water masses cannot be calculated at the same time with only these two parameters. So during the same time as the development of this theory, physical and chemical oceanographers also tried to add more parameters to the calculation and the Optimum Multi-parameter (OMP) analysis is one of the typical products.

Base on above results, Tomczak (1981) extended the analysis into more than three water masses by adding more parameters/water properties (such as phosphate and silicate) and solving the equations of linear mixing without assumptions. In Tomczak and Large (1989), this method was successfully applied to the analysis of mixing in the thermocline in Eastern Indian Ocean. As a summary and practical use of the above results, the Optimal Multivariable Parameter (OMP) analysis was developed and successfully applied in the analysis of water masses in specific regions (e.g. Karstensen and Tomczak, 1997, 1998a). Parameters (6 key water properties in our study) from the water samples are extracted and compared with SWTs of each water masses to identify their composition structure and percentage in detail.

Before we start the calculation of OMP analysis, some basic definitions of SWTs need to be reiterated again. SWTs are the origin water masses in their formation area and carry their own properties (Poole and Tomczak, 1999). During transport and



124 mixing on the pathway, the total amount of water properties remains constant. In a mixed product of two water masses,
125 contribution from each SWT can be calculated by using a linear set of mixing equations, if we know one water property
126 (such as salinity) in this mixed product and both SWTs. But only one property/parameter becomes insufficient if there are
127 three or more water masses mix together. As a result, we can calculate the percentages of each water mass in a final mixed
128 product with more water masses, with the essential prerequisite that the number of water masses not larger than the number
129 of variables plus one.

130 The theory and formulas in the OMP analysis are described in detail in Tomczak and Large (1989) and the website
131 <http://omp.geomar.de/>. Here we make a brief introduction to the OMP calculation that relates directly to our research, for
132 more details see the references above. OMP calculation is based on a simple model of linear mixing, assuming that all key
133 properties of water masses are affected by the same mixing process, and then to determine the distribution and of water
134 masses through the following linear equations.

135 **$Gx - d = R;$**

136 Where **G** is a parameter matrix of defined source water types (6 key properties in this study), **x** is a vector containing the
137 relative contributions of the water types to the sample (i.e. solution vector of the source water type fractions), **d** is a data
138 vector of water samples (observational data from GLODAPv2 in this study) and **R** is a vector of residual. The solution is to
139 find out the minimum the residual (**R**) with linear fit of parameters (key properties) for each data point with a non-negative
140 values.

141 Prerequisites (or restrictions) for using classic OMP is that source water types are defined closely enough to the
142 observational water samples with short transport times, so that the mixing can be assumed not influenced by biogeochemical
143 processes (i.e. consider all the parameters as quasi-conservative). Obviously, this prerequisite does not apply to our
144 investigation for the entire Atlantic scale, so we use the extended OMP analysis instead. The way of considering
145 biogeochemical processes is to convert non-conservative parameters (phosphate and nitrate) into conservative parameters by
146 introducing the "preformed" nutrients PO and NO, where PO and NO show the concentrations of Phosphate and Nitrate in
147 sea water by considering the consumption of dissolved Oxygen from respiration (in other words, the alteration due to
148 respiration is eliminated) (Broecker, 1974; Karstensen and Tomczak, 1998b).

149 **2.3. OMP runs in this study**

150 As mentioned in the companion paper (Liu and Tanhua, 2019) Source Water Types (SWTs) are the origin form of each
151 water mass in the formation area and we grasp the properties of main SWTs in the Atlantic Ocean. In this study, we show the
152 distributions of water masses in Atlantic Ocean after formations based on OMP analysis. The key properties of SWTs are
153 used in OMP analysis as the basis to determining the distributions of water masses.



154 In order to map all the distribution of water masses in the Atlantic we analyzed all the GLODAPv2 data in the Atlantic
 155 Ocean with OMP method by using 6 key properties from each water sample (potential temperature, salinity, oxygen, silicate,
 156 phosphate and nitrate). However some of these variables co-vary to some extent, in particular phosphate and nitrate, so that
 157 we have to control that in each OMP run we should have less than 6 water masses. Some regional factors should also be
 158 considered, as some water masses mix and new SWTs are formed during their mixing process. For example, LSW, ISOW
 159 and DSOW mix in the North Atlantic after leaving their formation area, as a result, SWTs of upper and lower NADW are
 160 formed. Here we specify some ‘mixing regions’ for these water masses. Between 40 and 60 °N, we define such a ‘mixing
 161 region’, since all the five water masses including already formed LSW, ISOW and DSOW and newly formed upper and
 162 lower NADW simultaneously exist. So in this region, key properties from all these five SWTs are used simultaneously in
 163 OMP runs. In south of 40 °N, only upper and lower NADW are used while north of 60 °N, only LSW, ISOW and DSOW are
 164 used. A similar situation exists in the South Atlantic where we consider south of 50 °S as another ‘mixing region’, since a
 165 new SWT of AABW is formed here due to the mixing of CDW and WSBW. So in this region, key properties from all the
 166 three SWTs are used in the OMP runs while in north of 50 °S, only AABW is used.

167 Consolidate the above reasons, and also consider the distribution of all the water masses, all the data in the Atlantic Ocean
 168 are divided into four, almost vertical, layers by potential density, since all the water masses distribute within their core layer
 169 and only mix with neighboring water masses at the boundary of each layer. In horizontal direction, Atlantic Ocean is
 170 manually divided into several horizontal sections in order to remove water masses that are not likely to appear in the area to
 171 avoid excessive (more than 6) water masses in each OMP run. The central layer is divided into two sections by 35 °N to
 172 distinguish SAIW and AAIW, which has similar properties. In the intermediate and deep layer, Atlantic Ocean is divided
 173 into three sections. The region north of 60 °N contains the LSW, ISOW and DSOW. From 40 to 60 °N is defined as mixing
 174 region. LSW, ISOW, DSOW mix with each other and finally form upper and lower NADW. As a result, all the five SWTs
 175 should be contained in one OMP runs in this section. And the third part, from 50 °S to 40 °N, only upper and lower NADW
 176 are considered. In high latitude region in South Atlantic, mixing region of CDW and WSBW is defined as south of 50 °S. In
 177 this mixing region, CDW, WSBW mix and AABW is formed, but no horizontal layer division in this area because the
 178 difference of density is not obvious. From north of 50°S only AABW are used in OMP runs until equator. In addition, for
 179 relative special long transport water masses those across the equator, AAIW upper and lower NADW, we do not subject to
 180 restrictions of equator.

181 This way we end up with a set of 13 different OMPs that are used for estimating the fraction of water masses in each water
 182 sample. The density and the latitude of the water sample is used to determine which IMP should be applied, Table 1. Note
 183 that all water masses are present in more than one OMP so that reasonable smooth (i.e. realistic) transitions between the
 184 different OMPs can be realized. However, it is unavoidable that there will occasionally be step-like features across the
 185 vertical and horizontal boundaries defined in Table 1.



186 3. Result: Distribution of water masses based on GLODAPv2

187 In this section, the horizontal and vertical distributions of the main water masses are displayed in different density layers. On
 188 the maps of horizontal view, water mass fractions are plotted at each station with the interpolated format at their core
 189 densities. In order to avoid large interpolation errors, a station is considered as without data and plotted as grey rather than
 190 colored dots if there is no data within $\pm 0.1 \text{ kg/m}^3$ from core density.

191 To exemplify the vertical distribution of the water masses we are also display sections from representative cruises. For this
 192 we use 5 selected WOCE/GO-SHIP cruises that together provide a reasonable representation of the Atlantic Ocean, as shown
 193 in Figure 2. These are the A16 cruise (Expocodes: 33RO20130803 & 33RO20131223) that is a meridional overview of all
 194 the main water masses in the Atlantic Ocean, and that was also used for the distribution of the properties in Figure 1. The
 195 A05 (Expocode: 74AB20050501) and A10 (Expocode: 33RO20110906) sections displays the zonal distribution of the water
 196 masses in the North (A05) and South (A10) Atlantic separately. The A25 (Expocode: 06MM20060523) section is located at
 197 a relative higher latitude region compared to the A05 section and better represent the deep and overflow waters in particular.
 198 From this cruise, we focus on the investigation of LSW, ISOW and DSOW, with the purpose to show origin of upper and
 199 lower NADW. The SR04 (Expocode: 06AQ20101128) on the other hand is a section in the Antarctic region near Weddell
 200 Sea with certain significance for the origin and formation of AABW. For each figure with horizontal distribution we also
 201 display a map with a cartoon of the main currents in that density layer and with the main formation region of each water
 202 mass indicated as striped boxes.

203 In this section horizontal and vertical distribution of all water masses discussed and defined in the companion paper (Liu and
 204 Tanhua, 2019) are displayed on maps and sections respectively. We start with the Upper Layer and work our way down the
 205 water column. In the Upper Layer ($\sigma_\theta < 27 \text{ kg/m}^3$ and mostly with depths above $\sim 500\text{-}1000\text{m}$), central waters are the
 206 dominate water masses in this layer, where we define four SWTs, ENACW, WNACW, ESACW and WSACW (see table 3
 207 in the companion paper, Liu and Tanhua, 2019 for definitions). Below the Upper Layer resides the Intermediate Layer (σ_θ
 208 between 27 and 27.7 kg/m^3 and mostly with depths between ~ 1000 and 2000m). In this layer, we have the following SWTs;
 209 SAIW from the north AAIW from the south and MOW from the east. The Deep Layer resides from ~ 2000 to 4000m and σ_θ
 210 between 27.7 and 27.88 kg/m^3 . The upper and lower NADW are two main SWTs in mid and low latitude region in this layer.
 211 Their origin, LSW, ISOW and DSOW will also be investigated in relative high latitude region. Both bottom waters are
 212 located in the Bottom Layer below 4000m with $\sigma_\theta > 27.88 \text{ kg/m}^3$. AABW and NEABW are two main water masses in this
 213 layer and have similar properties, especially high silicate. Traced back to the source, NEABW is a branch from AABW after
 214 passing the equator. After spanning most Atlantic there is a sharp reduction of silicate concentration this is the reason why
 215 we define a new SWT of NEABW.



216 3.1. The Upper Layer: ENACW, WNCAW, ESACW and WSCAW

217 The horizontal distributions of four main water masses in the Upper Layer are shown on the maps in Figure 3. In general,
218 eastern central waters, both for the northern and southern variation, have relative higher potential density and are located at
219 deeper depth (i.e. higher density) compared with western central waters. In spatially distribution, the East North Atlantic
220 Central Water (ENACW) is mainly located in the north east part of North Atlantic, near the formation area. The ENACW is
221 formed during winter subduction in the seas west of Iberian Peninsula and drifts to the south along the south branch of the
222 North Atlantic Current (McCartney and Talley, 1982) and mainly locates in north east part of North Atlantic, near the
223 formation area (Garcia-Ibanez et al., 2015; Talley and Raymer, 1982). The WNACW, which is formed at the south flank of
224 the Gulf Stream (Klein and Hogg, 1996), spreads along the North Atlantic Current and distributes in east-west band between
225 $\sim 10^\circ\text{N}$ and 40°N .

226 East South Atlantic Central Water (ESACW) distributes all over most South Atlantic and with lower percentages ($\sim 30\%$ --
227 40%) can also be found in the tropical and subtropical north Atlantic below (at higher densities) than the West North Atlantic
228 Central Water (WNACW). WNACW is located in north tropical and subtropical North Atlantic, where this water mass is
229 formed. West South Atlantic Central Water (WSACW) dominates the upper layer of South Atlantic, resides over ESACW
230 and can also be seen above ENACW in the North Atlantic. In the South Atlantic, our results are similar to those of
231 (Kirchner et al., 2009) that found that the WSACW and ESACW spread all over the South Atlantic, eastward along South
232 Atlantic Current, and then northwest along the Benguela Current and South Equator Current, and finally southward along
233 Brazilian Current. In general, both WSACW and ESACW dominate the central/upper layer in South Atlantic and across the
234 equator until $\sim 10^\circ\text{N}$.

235 The WSACW is formed in the region near the South America coast between 30 and 45°S , where surface South Atlantic
236 Current brings central water to the east (Kuhlbrodt et al., 2007). Formation of ESACW takes place in the eastern South
237 Atlantic Ocean close to the area southwest of South Africa (Deruijter, 1982; Lutjeharms and van Ballegooyen, 1988) and
238 spreads to the north along the Benguela Current (Peterson and Stramma, 1991).

239 From the A16 and A05 sections the meridional and zonal distribution of WNACW and ENACW, the both dominating
240 central water masses in North Atlantic, can be seen. The vertical distribution shows that the WNACW is located at lower
241 densities compared to the ENACW. In the zonal A05 section the difference between east and west of the Mid-Atlantic-Ridge
242 (MAR) is obvious; west of the MAR WNACW dominates the upper layer. Both thickness and percentage are significantly
243 larger than east, while the situation in east of MAR is the opposite, due to their distance from respective formation areas.
244 ENACW is located at the upper $\sim 500\text{m}$ — 1000m below WNACW and over SAIW and MOW.

245 The vertical distribution of WSACW and ESACW based on A16 and A10 sections has similarities to the north central waters
246 where the western variety is located at lower densities compared to the eastern variety. The distribution of WSACW and
247 ESACW can be clearly seen by Figure 4 including their transports to the north that can be clearly seen by the A16 section. In



248 contrast to the north Atlantic the difference between east and west of the MAR, as seen in the A10 section, is not clear
249 compared with the A05 section for the North Atlantic.

250 3.2. The Intermediate Layer: AAIW, SAIW and MOW

251 In the intermediate layer (σ_θ between 27 and 27.7 kg/m³) three water masses can be considered as dominating. Two of them,
252 the Subarctic Intermediate Water (SAIW) and the Mediterranean Overflow Water (MOW), show Northwest-Southeast
253 distinction in their distribution in the North Atlantic although with similar densities. The SAIW is located in north of 40 °N
254 with higher percentages in the western part while the MOW is mainly distributed in the region east of the Mid-Atlantic-
255 Ridge, which is consistent with results from (Read, 2000). The third water mass, the AAIW, has a southern origin and is
256 found at lighter densities, Figure 5

257 In the South Atlantic, AAIW is the only water mass that originates from the south hemisphere in the Intermediate Layer and has
258 the lowest potential density (main core with potential density ~27.2 kg/m³) of these three water masses. The AAIW
259 originates from the surface layer (upper 200m) north of the Antarctic Circumpolar Current (ACC) and east of Drake Passage
260 (Alvarez et al., 2014; McCartney, 1982). Most AAIW is formed in the region south of 40 °S where it sinks and spreads to
261 the north at pressures between ~1000 and 2000db at potential densities between 27.0 and 27.7 kg/m³ (Talley, 1996).

262 On the map, the spread of AAIW covers most of the Atlantic Ocean until ~40 °N and the percentage shows a decrease trend
263 to the north (Kirchner et al., 2009). The AAIW shows a general distribution within the intermediate layer based on potential
264 density (σ_θ) between 27.0 and 27.7 kg/m³, Figure 7. At ~40 °S, upper NADW injects into the space between AAIW and
265 AABW (Figure 12) and all the three water masses mix with each other in this area. From the observations on the meridional
266 A16 section, the AAIW spreads northward after leaving the formation area, across the equator and further north until ~40
267 °N, where it meets MOW and SAIW. The upper boundary between AAIW and central waters (ENACW and ESACW) are
268 mostly along the potential density line $\sigma_\theta = 27.7$ kg/m³. Based on A10 section the zonal distribution of AAIW is consistent
269 with the results A16 section and is the dominating intermediate water mass in the South Atlantic.

270 The SAIW, as one of the main intermediate water mass in North Atlantic, originates from the surface layer of the western
271 boundary of the North Atlantic Subpolar Gyre, sinks and spreads along the Labrador Current, crossing the MAR in the
272 region north of 40 °N (Lazier and Wright, 1993; Pickart et al., 1997).

273 From the A16 section, only some light trace of SAIW in the north can be found since this cruise in 2013 was distance away
274 from the formation area of SAIW in northwest Atlantic. On the zonal A05 section SAIW is a dominating intermediate water
275 mass above the LSW, Figure 6, particularly in the western basin since SAIW originates in the west.



276 MOW is another main intermediate water mass that is present in the North Atlantic. This water mass overflows from Strait
277 of Gibraltar at $\sim 40^\circ\text{N}$ and spreads in two branches to the north and the west (Price et al., 1993). The MOW originates from
278 the east in the Gulf of Cadiz where Mediterranean Water exits the Strait of Gibraltar as a deep current and then turns into
279 two branches after leaving the formation area near. One branch spreads to the north into the West European Basin until
280 $\sim 50^\circ\text{N}$, the other branch spreads to the west until, and past, the Mid-Atlantic-Ridge.

281 From the A16 section the MOW can be found between ~ 20 and 50°N , surrounded by ENACW from the top, SAIW from the
282 north, AAIW from the south and upper NADW from bottom. The observations from the A05 section shows that the MOW
283 flows from the east and spreads westwards until passing the MAR. East of the MAR the trace of MOW is clear, particularly
284 in the region close the Strait of Gibraltar.

285 3.3. The Deep and Overflow Layer: upper and lower NADW, LSW, ISOW and DSOW

286 As one of the main components of the thermohaline circulation in Atlantic Ocean, formation and distribution of North
287 Atlantic Deep Water (NADW) is the focus of several studies. NADW is the only main water mass that dominates the deep
288 and overflow layer with potential density (σ_θ) between 27.70 and 27.88 kg/m^3 and can be divided into two portions (upper
289 and lower) due to different properties and origins (Smethie and Fine, 2001). In this section, both portions, together with their
290 origins, are analyzed as independent water masses separately.

291 In the deep and overflow layer three water masses dominate the region north of 40°N , Figure 7: Labrador Sea Water (LSW),
292 Iceland-Scotland Overflow Water (ISOW) and Denmark Strait Overflow Water (DSOW). They are considered as the origin
293 of North Atlantic Deep Water (NADW). In the region south from 40°N the upper and lower NADW, considered as products
294 from the original three overflow water masses, can be found all over the Atlantic Ocean in the deep and overflow layer.

295 The Labrador Sea Water (LSW) is formed in the region of Labrador Sea by deep convection during winter (Clarke and
296 Gascard, 1983), and is typically found at mid-depth with $\sigma_\theta = \sim 27.77 \text{ kg/m}^3$. This water mass was noted by (Wüst and
297 Defant, 1936) due to its salinity minimum and later defined and named by Smith et al. (1937). Since then, with the
298 deepening of research on this water mass, the character was discovered as a contribution to the driving mechanism of
299 northward heat transport in the Atlantic Meridional Overturning Circulation (AMOC) (Rhein et al., 2011). In the specific
300 study on this water mass, LSW is divided into two units, ‘upper’ and ‘classic’, based on the differences in temperature and
301 salinity (Kieke et al., 2007; Kieke et al., 2006). In the large scale as throughout the whole Atlantic Ocean, LSW is still
302 treated as a unified water mass and considered as the main origin of upper NADW (Elliot et al., 2002; Talley and McCartney,
303 1982). In the general scale, LSW distributes in the western part of the North Atlantic in Labrador Sea and Irminger Sea
304 region and the distribution is influenced by the Gulf Stream, the Labrador Current and the North Atlantic Current (Elliot et
305 al., 2002; Talley and McCartney, 1982).



306 Seen from the aerial view of the analysis results to the whole GLODAPv2 dataset, Figure 8, LSW mainly distributes in the
 307 Northwest Atlantic north 40 °N near the Labrador Sea and Irminger Basin with core at $\sigma_\theta = \sim 27.77 \text{ kg/m}^3$. In terms of
 308 vertical distribution, A25 cruise (Expocode: 06MM20060523) shows that LSW dominates the depth between 500 and
 309 2000m, and meanwhile, the fraction decreases with the spatial change to the east (direction to Iberian Peninsula) thus far
 310 away from the formation area (Greenland). This distribution is basically consistent with historical literatures. After
 311 southward transport with Labrador Current, LSW spreads eastward with Gulf Stream and North Atlantic Current until it
 312 meets MOW. In general, LSW is the dominate mid-depth water mass in the region north of 40 °N in Northwest Atlantic.
 313 The Iceland–Scotland Overflow Water (ISOW) and Denmark Strait Overflow Water (DSOW), as original water masses that
 314 contribute to the formation of the lower NADW (Read, 2000), are located in the west and east part of North Atlantic (north
 315 of 40 °N) respectively with the main core near $\sigma_\theta = 27.88 \text{ kg/m}^3$. Both ISOW and DSOW are formed by water masses from
 316 the Arctic Ocean and the Nordic Seas those reach the North Atlantic Ocean (Lacan and Jeandel, 2004; Tanhua et al., 2005).
 317 As an indispensable link of the thermohaline circulation, the southward outflow of ISOW and DSOW to the Atlantic Ocean
 318 plays an important role, as well as LSW, in the deep-water component of the AMOC and has certain a certain impact on the
 319 European and even the global climate.

320 In general, ISOW is formed in the regions of Greenland, Iceland and Norwegian Seas, outflows southward in the west of
 321 Iceland, across the Faeroe Bank Channel into the eastern part of North Atlantic Ocean (Kissel et al., 1997; Swift, 1984).
 322 From a more specific perspective, ISOW has two branches. One branch passes near the Charlie-Gibbs Fracture Zone
 323 (CGFZ) and flow into Irminger basin at densities above the DSOW. The other branch goes southward into the West
 324 European Basin and meets the Northeast Atlantic Bottom Water (NEABW) (Garcia-Ibanez et al., 2015).

325 Consistent with literatures, the top view distribution from map shows ISOW mainly distributes in the Northeast Atlantic
 326 north 40 °N between Iceland and Iberian Peninsula with core at $\sigma_\theta = \sim 27.88 \text{ kg/m}^3$. In terms of vertical distribution, the A25
 327 section shows that ISOW outflows at east of Iceland across Iceland-Faroe Ridge with core at depth between ~ 2000 and
 328 3000m. In west of Iceland, ISOW can also be found in the Denmark Strait, where core of DSOW is located, with low
 329 fraction.

330 DSOW is the water mass that overflows through the Denmark Strait in west of Iceland and into Irminger Basin and Labrador
 331 Sea with $\sigma_\theta = \sim 27.88 \text{ kg/m}^3$ (Tanhua et al., 2005). This overflow water mass is considered as the coldest and densest
 332 component of the sea water in the Northwest Atlantic Ocean and constitute a significant part of the southward flowing
 333 NADW (Swift, 1980). Compositions of DSOW can be traced to many surrounding water masses. Besides Arctic
 334 Intermediate Water (AIW), Re-circulating Atlantic Water (RAW), Polar Surface Water (PSW) and Arctic Atlantic Water
 335 (AAW) are all considered to be parts of the source (Clarke et al., 1990; Smethie Jr, 1993; Swift, 1980; Tanhua et al., 2005).
 336 Rudels et al. (2002) noted the contribution from East Greenland Current (EGC) to the DSOW, EGC that brings Arctic Water



in deep layer through the Fram Strait into the Greenland Sea is known as the main mechanism of forming DSOW and this provided us a theoretical basis for determining the distribution of DSOW.

According to the OMP calculations, and also referring to the above literature, the following conclusions about DSOW can be drawn. In the horizontal direction, map distribution shows DSOW mainly distributes along the drainage area of EGC with $\sigma_\theta = \sim 27.88 \text{ kg/m}^3$. DSOW starts from the Greenland Sea, southward flows into the Irminger Sea along EGC and then westward into Labrador Sea. The vertical distribution based on the A25 section shows that DSOW overflows through the Greenland-Scotland Ridge close proximity to the continental slope with core at depth between ~ 2500 and 3000m . Compared with ISOW, pathway of DSOW is relative narrow and limited within the eastern bottom in the Irminger Basin.

Main cores of ISOW and DSOW can be seen in both sides of Iceland separately below LSW. ISOW distributes all over the region between Greenland and Iberian Peninsula. After passing the Iceland, ISOW and DSOW convergence into one share and spread further southward. All the three water masses, LSW ISOW and DSOW, origin from the North Atlantic region, spread southward and finally become the dominate water masses in deep and overflow layer. Considering the change of properties during the pathway, especially the final product of mixing compared with original ISOW and DSOW, also in order to comply with the needs of large-scale distribution in Atlantic Ocean and without paying too much attention to these details, two new water masses, upper and lower NADW based on SWTs in the companion paper (Liu and Tanhua, 2019), are adopted in the main Atlantic region south of 40°N , whereas LSW ISOW and DSOW are not used in the OMP analysis and replaced upper and lower NADW.

After passing 40°N , upper and lower NADW, considered as independent water masses, continue to spread until $\sim 50^\circ\text{S}$ and dominate the most Atlantic Ocean in this layer. During the process to the south, NADW is transported along Deep West Boundary Current (DWBC) and also eastward with eddies (Lozier, 2012).

The OMP analysis shows that the upper and lower NADW are the main water masses in Deep and Overflow Layer, Figure 9. As the productions and considered as independent water masses, upper NADW distributes at a relative shallow pressure, while lower NADW with higher pressure close to their original water masses. After molding, upper and lower NADW are formed and spread southward with DWBC along the continental slope also spreads eastward and cover mostly all over the Atlantic Ocean in this layer due to eddies during the pathway (Lozier, 2012).

In horizontal scale, the map view shows that upper NADW covers the most area of deep and overflow layer, while lower NADW is found with higher fractions in the west region near the Deep Western Boundary Current (DWBC), especially in South Atlantic. In the vertical scale based on observation from meridional (A16) and zonal (A05 and A10) cruises, relative thicker lower NADW than upper NADW are discovered. Upper NADW, due to lower potential density, lies over lower NADW during the whole way to the south with their boundary at $\sim 2000\text{m}$ depth. The boundary between upper NADW and



intermediate water masses, AAIW and SAIW, are almost along our definition line ($\sigma_\theta = 27.7 \text{ kg/m}^3$). AABW is the only bottom water mass that contacts with upper NADW. In the region south of 40°S , upper NADW is deflected up after it meets AABW and high mixing happens in this region due to ACC. Lower NADW is seen south to $\sim 40^\circ\text{S}$ where it meets AABW.

3.4. The Bottom Layer: AABW and NEABW

AABW and NEABW dominate the bottom layer ($\sigma_\theta > 27.88 \text{ kg/m}^3$). In fact, both water masses have the same origin but distinguished by defining a new SWT as NEABW due to the sharp reduction of silicate, which is an important signal to label bottom water masses, after passing the equator. From aerial view of the maps, Figure 10, AABW and NEABW cover the most bottom area of South and North Atlantic respectively.

The AABW is formed in the Weddell Sea region south of the Antarctic Circumpolar Current (ACC). After leaving the formation area, AABW sinks to the bottom due to the high density during the way north. After passing the ACC, AABW meets NADW and they have some water exchange from 50°S until AABW reaches the equator (van Heuven et al., 2011). Due to dramatical change of properties after passing the equator, especially the sudden decrease of silicate, AABW is redefined as a new SWT, NEABW, in the north of equator. In the north of equator, water mass of NEABW origins from the newly defined SWT of NEWBW and as actually a continuation of AABW, becomes the dominate bottom water. Similar with AABW, NEABW also mainly mixed with lower NADW between equator and 40°N . In north of 40°N , NEABW spreads further north until $\sim 50^\circ\text{N}$, where it meets lower NADW origins from ISOW (Garcia-Ibanez et al., 2015).

In the A16 section in Figure 11, AABW sinks to the bottom between $\sim 50 - 60^\circ\text{S}$ and spreads north to equator in the bottom layer below 4000m ($\sigma_\theta > 27.88 \text{ kg/m}^3$). After passing the ACC at $\sim 40^\circ\text{S}$, AABW meets upper NADW that is, in general, deflected upwards. During this process, part of AABW penetrate into the Deep and Overflow Layer (σ_θ between 27.7 and 27.88 kg/m^3), so $\sim 20 - 50\%$ of AABW can be seen in this layer in both the meridional (A16) and the zonal (A10) section. In the further north region, between 40°S and the equator, AABW contacts mainly with lower NADW instead of upper NADW. The fraction of AABW also increases with pressure. North of equator, NEABW is the only bottom water mass and distributes in the bottom in both sides of the MAR with the main core located below $\sim 4000\text{m}$ with $\sigma_\theta > 27.88 \text{ kg/m}^3$. Observations from the A16 and A05 sections show NEABW in contact with lower NADW from the above and the fraction of NEABW increases with depth.

3.5. The Southern Water masses: WSBW, CDW, and AABW

In this section the formation of AABW in the Weddell Sea Region is investigated and displayed, Figure 12. Similarly to the situation of NADW, AABW originates from two initial water masses, CDW and WSBW in the Antarctic region. An additional section, SR04 is analyzed to display the detail about formation of AABW. The SR04 section in the Weddell Sea region is formed by two parts representing the formation of AABW in both the meridional and zonal directions.



397 In the zonal section across the Weddell Sea, AABW can be seen as the product from two original water masses, CDW and
398 WSBW. The core of CDW distributes in the upper 1000m and WSBW origins at the surface and subducts along the
399 continental slope into the bottom below 4000m. This result is consistent with (van Heuven et al., 2011). Both original water
400 masses meet each other at depth between ~2000 and 4000m, where AABW is formed with main core locates at ~3000m.

401 The meridional section of SR04 cruise shows the northward outflow of AABW into the Atlantic Ocean. AABW is located
402 between 2000 and 4000m, as a product from CDW and WSBW. After leaving Weddell Sea region, AABW is considered as
403 an independent water mass from north of 60 °S and spreads further northward as the only bottom water mass until the
404 equator. In relative low latitude region (north of 60 °S), AAIW can also be found in shallow layer, since here is the boundary
405 between formation area of AAIW and AABW.

406 **4. Conclusion and Discussion**

407 In this study, the distributions of water masses in Atlantic Ocean are investigated based on the GLODAPv2 dataset and the
408 definition of water masses presented by (Liu and Tanhua, 2019). We have shown maps and sections of water mass
409 distribution through the Atlantic Ocean basin. Water masses are mostly distributed within the density layer where they are
410 formed, and mixing of water masses away from their formation areas are evident..

411 The central water masses, ENACW WNACW ESACW and WSACW, occupy the upper/central layer of the Atlantic Ocean
412 by following the dividing line $\sigma_\theta < 27 \text{ kg/m}^3$ and high salinity is also one significant property to identity them. Below the
413 Upper layer, SAIW and MOW are the two main water masses in the intermediate layer in North Atlantic. SAIW comes from
414 the northwest, sinks during the way to the southeast. In the eastern part, MOW overflows from the Mediterranean Sea, across
415 the Strait of Gibraltar and spreads to the north and west. The most significant property of MOW is high salinity at around
416 1000m depth. In the South Atlantic, AAIW is the dominate water mass in intermediate layer. After the formation in the
417 shallow layer, AAIW sinks into intermediate depth (around 1000m) and spreads to the north until ~ 40 °N and this water
418 mass can easily be found with low salinity.

419 NADW is the main water mass in the Deep and Overflow Layer. In order to show more clearly the distribution of water
420 masses in this layer, more detail are investigated to display upper and lower NADW, as well as their origin, LSW, ISOW and
421 DSOW, separately.

422 For the bottom waters, AABW and NEABW, have similar properties, especially high silicate content, since NEABW, traced
423 back to the source, is a branch from AABW after passing the equator. After spanning most Atlantic there is a sharp reduction
424 of silicate concentration, the new defined SWT, NEABW becomes the dominate water mass in the bottom.

425



426 Acknowledgements

427 This work is based on the comprehensive and detailed data from GLODAP data set throughout the past few decades and we
428 would like to thank the efforts from all the scientists and crews on cruises and the working groups of GLODAP for their
429 contributions and selfless sharing. In particular, we are grateful to the theoretical and technical support from J. Karstensen
430 and M. Tomczak for the OMP analysis. Thanks to the China Scholarship Council (CSC) for providing funding support to
431 Mian Liu's PhD study in GEOMAR Helmholtz Centre for Ocean Research Kiel.

432 References

- 433 Alvarez, M., Brea, S., Mercier, H., Alvarez-Salgado, X.A.: Mineralization of biogenic materials in the water masses of the
434 South Atlantic Ocean. I: Assessment and results of an optimum multiparameter analysis. *Prog Oceanogr* 123, 1-23, 2014.
- 435 Broecker, W.S.: No a Conservative Water-Mass Tracer. *Earth Planet Sc Lett* 23, 100-107, 1974.
- 436 Carracedo, L., Pardo, P.C., Flecha, S., Pérez, F.F.: On the Mediterranean Water Composition. *Journal of Physical*
437 *Oceanography* 46, 1339-1358, 2016.
- 438 Clarke, R.A., Giscard, J.-C.: The Formation of Labrador Sea Water. Part I: Large-Scale Processes. *Journal of Physical*
439 *Oceanography* 13, 1764-1778, 1983.
- 440 Clarke, R.A., Swift, J.H., Reid, J.L., Koltermann, K.P.: The formation of Greenland Sea Deep Water: double diffusion or
441 deep convection? *Deep Sea Research Part A. Oceanographic Research Papers* 37, 1385-1424, 1990.
- 442 Deruijter, W.: Asymptotic Analysis of the Agulhas and Brazil Current Systems. *Journal of Physical Oceanography* 12, 361-
443 373, 1982.
- 444 Elliot, M., Labeyrie, L., Duplessy, J.C.: Changes in North Atlantic deep-water formation associated with the Dansgaard-
445 Oeschger temperature oscillations (60-10 ka). *Quaternary Science Reviews* 21, 1153-1165, 2002.
- 446 Emery, W.J., Meincke, J.: Global Water Masses - Summary and Review. *Oceanologica Acta* 9, 383-391, 1986.
- 447 Fyfe, J.C., Saenko, O.A., Zickfeld, K., Eby, M., Weaver, A.J.: The role of poleward-intensifying winds on Southern Ocean
448 warming. *Journal of Climate* 20, 5391-5400, 2007.
- 449 Garcia-Ibanez, M.I., Pardo, P.C., Carracedo, L.I., Mercier, H., Lherminier, P., Rios, A.F., Perez, F.F.: Structure, transports
450 and transformations of the water masses in the Atlantic Subpolar Gyre. *Prog Oceanogr* 135, 18-36, 2015.
- 451 Hinrichsen, H.H., Tomczak, M.: Optimum multiparameter analysis of the water mass structure in the western North Atlantic
452 Ocean. *Journal of Geophysical Research: Oceans* 98, 10155-10169, 1993.
- 453 Ishii, M., Suzuki, T., Key, R.: Pacific Ocean Interior Carbon Data Synthesis, PACIFICA, in Progress. *PICES Press* 19, 20,
454 2011.
- 455 Karstensen, J., Stramma, L., Visbeck, M.: Oxygen minimum zones in the eastern tropical Atlantic and Pacific oceans. *Prog*
456 *Oceanogr* 77, 331-350, 2008.



- 457 Karstensen, J., Tomczak, M.: Ventilation processes and water mass ages in the thermocline of the southeast Indian Ocean.
458 Geophysical Research Letters 24, 2777-2780, 1997.
- 459 Karstensen, J., Tomczak, M.: Age determination of mixed water masses using CFC and oxygen data. Journal of Geophysical
460 Research: Oceans 103, 18599-18609, 1998a.
- 461 Karstensen, J., Tomczak, M.: Age determination of mixed water masses using CFC and oxygen data. J Geophys Res-Oceans
462 103, 18599-18609, 1998b.
- 463 Key, R.M., Kozyr, A., Sabine, C.L., Lee, K., Wanninkhof, R., Bullister, J.L., Feely, R.A., Millero, F.J., Mordy, C., Peng,
464 T.H.: A global ocean carbon climatology: Results from Global Data Analysis Project (GLODAP). Global biogeochemical
465 cycles 18, 2004.
- 466 Key, R.M., Tanhua, T., Olsen, A., Hoppema, M., Jutterström, S., Schirnack, C., van Heuven, S., Kozyr, A., Lin, X., Velo, A.,
467 Wallace, D.W.R., Mintrop, L.: The CARINA data synthesis project: introduction and overview. Earth Syst. Sci. Data 2, 105-
468 121, 2010.
- 469 Kieke, D., Rhein, M., Stramma, L., Smethie, W.M., Bullister, J.L., LeBel, D.A.: Changes in the pool of Labrador Sea Water
470 in the subpolar North Atlantic. Geophysical Research Letters 34, 2007.
- 471 Kieke, D., Rhein, M., Stramma, L., Smethie, W.M., LeBel, D.A., Zenk, W.: Changes in the CFC inventories and formation
472 rates of Upper Labrador Sea Water, 1997-2001. Journal of Physical Oceanography 36, 64-86, 2006.
- 473 Kirchner, K., Rhein, M., Huttel-Kabus, S., Boning, C.W.: On the spreading of South Atlantic Water into the Northern
474 Hemisphere. J Geophys Res-Oceans 114, 2009.
- 475 Kissel, C., Laj, C., Lehman, B., Labyrie, L., Bout-Roumazelles, V.: Changes in the strength of the Iceland-Scotland
476 Overflow Water in the last 200,000 years: Evidence from magnetic anisotropy analysis of core SU90-33. Earth Planet Sc
477 Lett 152, 25-36, 1997.
- 478 Klein, B., Hogg, N.: On the variability of 18 Degree Water formation as observed from moored instruments at 55 degrees W.
479 Deep-Sea Research Part I-Oceanographic Research Papers 43, 1777-&,1996.
- 480 Klein, B., Tomczak, M.: Identification of diapycnal mixing through optimum multiparameter analysis: 2. Evidence for
481 unidirectional diapycnal mixing in the front between North and South Atlantic Central Water. Journal of Geophysical
482 Research: Oceans 99, 25275-25280, 1994.
- 483 Kuhlbrodt, T., Griesel, A., Montoya, M., Levermann, A., Hofmann, M., Rahmstorf, S.: On the driving processes of the
484 Atlantic meridional overturning circulation. Reviews of Geophysics 45, 2007.
- 485 Lacan, F., Jeandel, C.: Neodymium isotopic composition and rare earth element concentrations in the deep and intermediate
486 Nordic Seas: Constraints on the Iceland Scotland Overflow Water signature. Geochemistry Geophysics Geosystems 5, 2004.
- 487 Lauvset, S.K., Key, R.M., Olsen, A., van Heuven, S., Velo, A., Lin, X., Schirnack, C., Kozyr, A., Tanhua, T., Hoppema, M.,
488 Jutterström, S., Steinfeldt, R., Jeansson, E., Ishii, M., Perez, F.F., Suzuki, T., Watelet, S.: A new global interior ocean
489 mapped climatology: the $1^\circ \times 1^\circ$ GLODAP version 2. Earth Syst. Sci. Data 8, 325-340, 2016.
- 490 Lazier, J.R.N., Wright, D.G.: Annual Velocity Variations in the Labrador Current. Journal of Physical Oceanography 23,
491 659-678, 1993.



- 492 Lozier, M.S.: Overturning in the North Atlantic. *Ann Rev Mar Sci* 4, 291-315, 2012.
- 493 Lutjeharms, J.R., van Ballegooyen, R.C.: Anomalous upstream retroflexion in the agulhas current. *Science* 240, 1770, 1988.
- 494 Mackas, D.L., Denman, K.L., Bennett, A.F.: Least squares multiple tracer analysis of water mass composition. *Journal of*
495 *Geophysical Research: Oceans* 92, 2907-2918, 1987.
- 496 McCartney, M.S.: The subtropical recirculation of Mode Waters. *J Mar Res* 40, 427-464, 1982.
- 497 McCartney, M.S., Talley, L.D.: The subpolar mode water of the North Atlantic Ocean. *Journal of Physical Oceanography*
498 12, 1169-1188, 1982.
- 499 Peterson, R.G., Stramma, L.: Upper-Level Circulation in the South-Atlantic Ocean. *Prog Oceanogr* 26, 1-73, 1991.
- 500 Pickart, R.S., Spall, M.A., Lazier, J.R.N.: Mid-depth ventilation in the western boundary current system of the sub-polar
501 gyre. *Deep-Sea Research Part I-Oceanographic Research Papers* 44, 1025-+, 1997.
- 502 Poole, R., Tomczak, M.: Optimum multiparameter analysis of the water mass structure in the Atlantic Ocean thermocline.
503 *Deep-Sea Research Part I-Oceanographic Research Papers* 46, 1895-1921, 1999.
- 504 Price, J.F., Baringer, M.O., Lueck, R.G., Johnson, G.C., Ambar, I., Parrilla, G., Cantos, A., Kennelly, M.A., Sanford, T.B.:
505 Mediterranean outflow mixing and dynamics. *Science* 259, 1277-1282, 1993.
- 506 Read, J.: CONVEX-91: water masses and circulation of the Northeast Atlantic subpolar gyre. *Prog Oceanogr* 48, 461-510,
507 2000.
- 508 Rhein, M., Kieke, D., Huttel-Kabus, S., Roessler, A., Mertens, C., Meissner, R., Klein, B., Boning, C.W., Yashayaev, I.: Deep
509 water formation, the subpolar gyre, and the meridional overturning circulation in the subpolar North Atlantic. *Deep-Sea*
510 *Research Part II-Topical Studies in Oceanography* 58, 1819-1832, 2011.
- 511 Rudels, B., Fahrbach, E., Meincke, J., Budéus, G., Eriksson, P.: The East Greenland Current and its contribution to the
512 Denmark Strait overflow. *ICES Journal of Marine Science* 59, 1133-1154, 2002.
- 513 Smethie Jr, W.M.: Tracing the thermohaline circulation in the western North Atlantic using chlorofluorocarbons. *Prog*
514 *Oceanogr* 31, 51-99, 1993.
- 515 Smethie, W.M., Fine, R.A.: Rates of North Atlantic Deep Water formation calculated from chlorofluorocarbon inventories.
516 *Deep-Sea Research Part I-Oceanographic Research Papers* 48, 189-215, 2001.
- 517 Smith, E.H., Soule, F.M., Mosby, O.: The Marion and General Greene Expeditions to Davis Strait and Labrador Sea, Under
518 Direction of the United States Coast Guard: 1928-1931-1933-1934-1935: Scientific Results, Part 2: Physical Oceanography.
519 US Government Printing Office, 1937.
- 520 Stramma, L., England, M.H.: On the water masses and mean circulation of the South Atlantic Ocean. *J Geophys Res-Oceans*
521 104, 20863-20883, 1999.
- 522 Sverdrup: *The Oceans: Their Physics, Chemistry and General Biology*, 1942.
- 523 Swift, J.H.: The Circulation of the Denmark Strait and Iceland Scotland Overflow Waters in the North-Atlantic. *Deep-Sea*
524 *Research Part a-Oceanographic Research Papers* 31, 1339-1355, 1984.



- 525 Swift, S.M.: Activity patterns of pipistrelle bats (*Pipistrellus pipistrellus*) in north- east Scotland. *Journal of Zoology* 190,
526 285-295, 1980.
- 527 Talley, L.: Antarctic intermediate water in the South Atlantic, *The South Atlantic*. Springer, pp. 219-238, 1996.
- 528 Talley, L., Raymer, M.: Eighteen degree water variability. *J. Mar. Res* 40, 757-775, 1982.
- 529 Talley, L.D., McCartney, M.S.: Distribution and Circulation of Labrador Sea-Water. *Journal of Physical Oceanography* 12,
530 1189-1205, 1982.
- 531 Tanhua, T., Olsson, K.A., Jeansson, E.: Formation of Denmark Strait overflow water and its hydro-chemical composition.
532 *Journal of Marine Systems* 57, 264-288, 2005.
- 533 Tomczak, M.: A multi-parameter extension of temperature/salinity diagram techniques for the analysis of non-isopycnal
534 mixing. *Prog Oceanogr* 10, 147-171, 1981.
- 535 Tomczak, M., Large, D.G.: Optimum multiparameter analysis of mixing in the thermocline of the eastern Indian Ocean.
536 *Journal of Geophysical Research: Oceans* 94, 16141-16149, 1989.
- 537 van Heuven, S.M.A.C., Hoppema, M., Huhn, O., Slagter, H.A., de Baar, H.J.W.: Direct observation of increasing CO₂ in the
538 Weddell Gyre along the Prime Meridian during 1973–2008. *Deep Sea Research Part II: Topical Studies in Oceanography* 58,
539 2613-2635, 2011.
- 540 Weiss, R.F., Ostlund, H.G., Craig, H.: Geochemical Studies of the Weddell Sea. *Deep-Sea Research Part a-Oceanographic*
541 *Research Papers* 26, 1093-1120, 1979.
- 542 Wüst, G., Defant, A.: *Atlas zur Schichtung und Zirkulation des Atlantischen Ozeans: Schnitte und Karten von Temperatur,*
543 *Salzgehalt und Dichte*. W. de Gruyter, 1936.
- 544
- 545

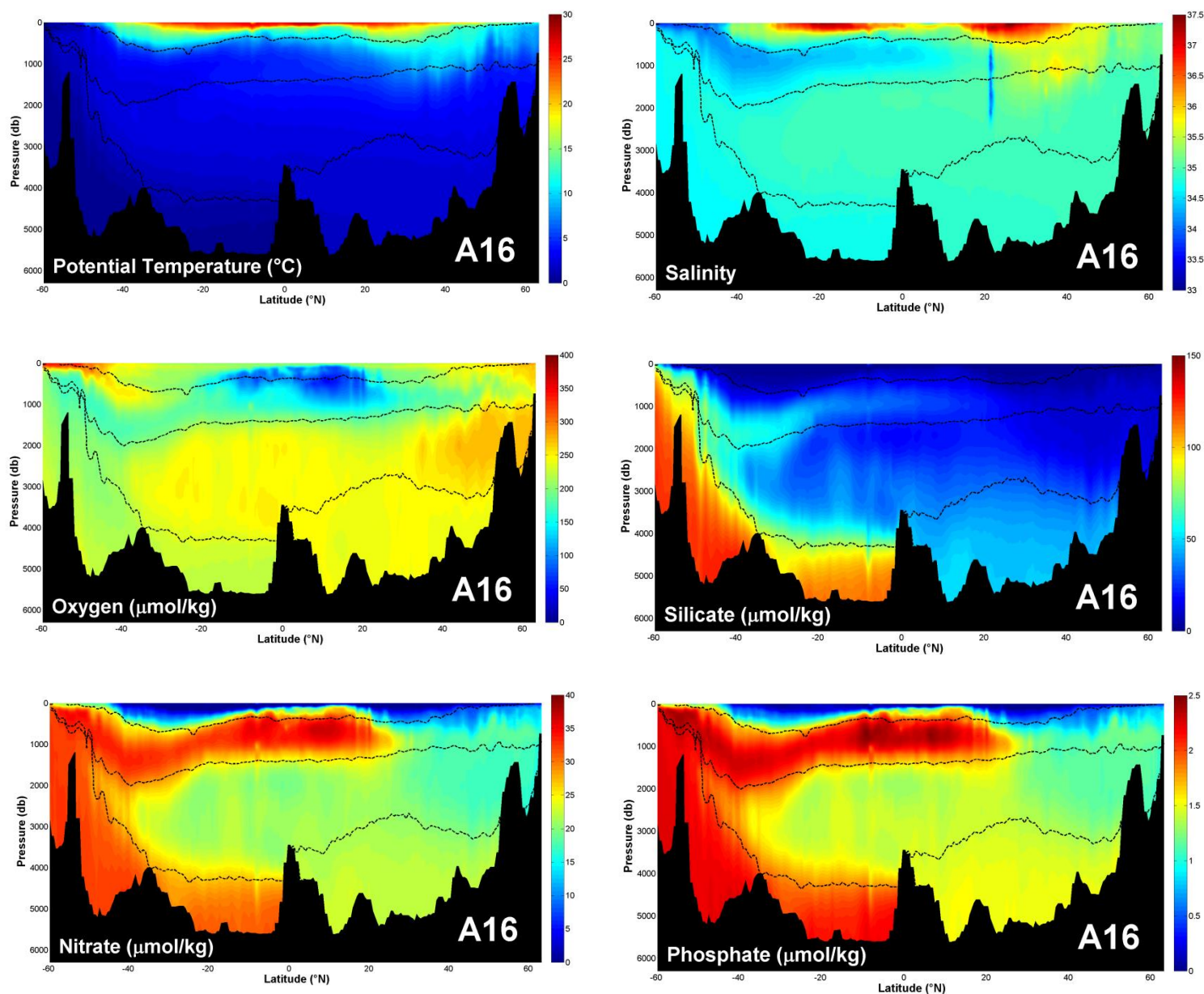


Fig 1 Key properties required by OMP analysis based on A16 cruises in 2013

Expocode: 33RO20130803 in North Atlantic & 33RO20131223 in South Atlantic

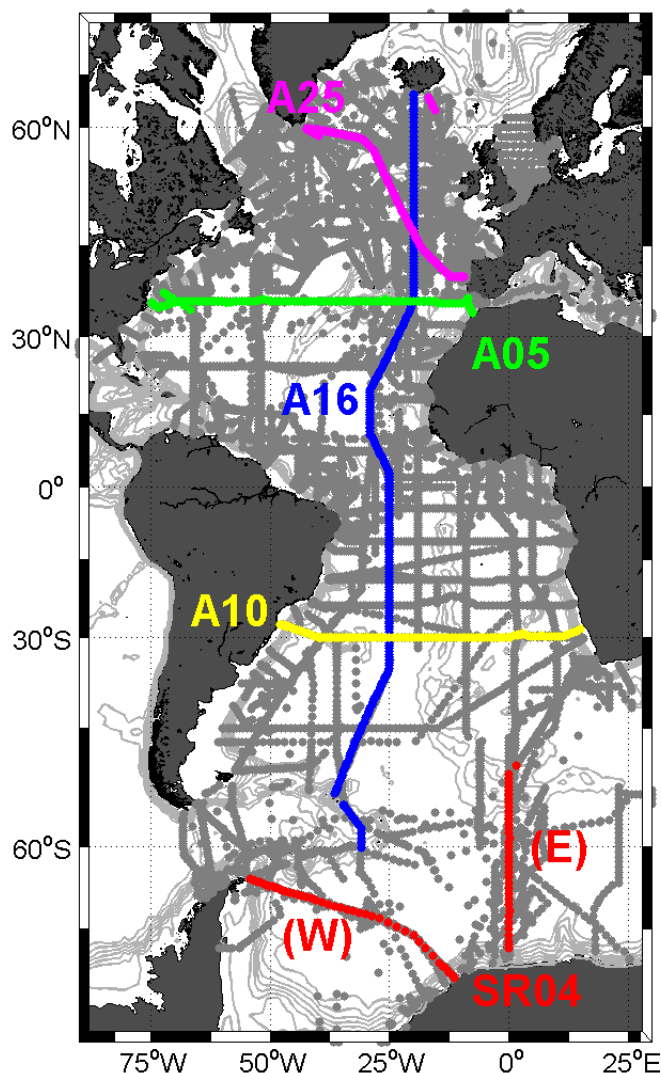


Fig 2 Maps of Cruises

Color lines show representative cruises analyzed in this paper while gray dots show all the GLODAPv2 stations

546

547



548

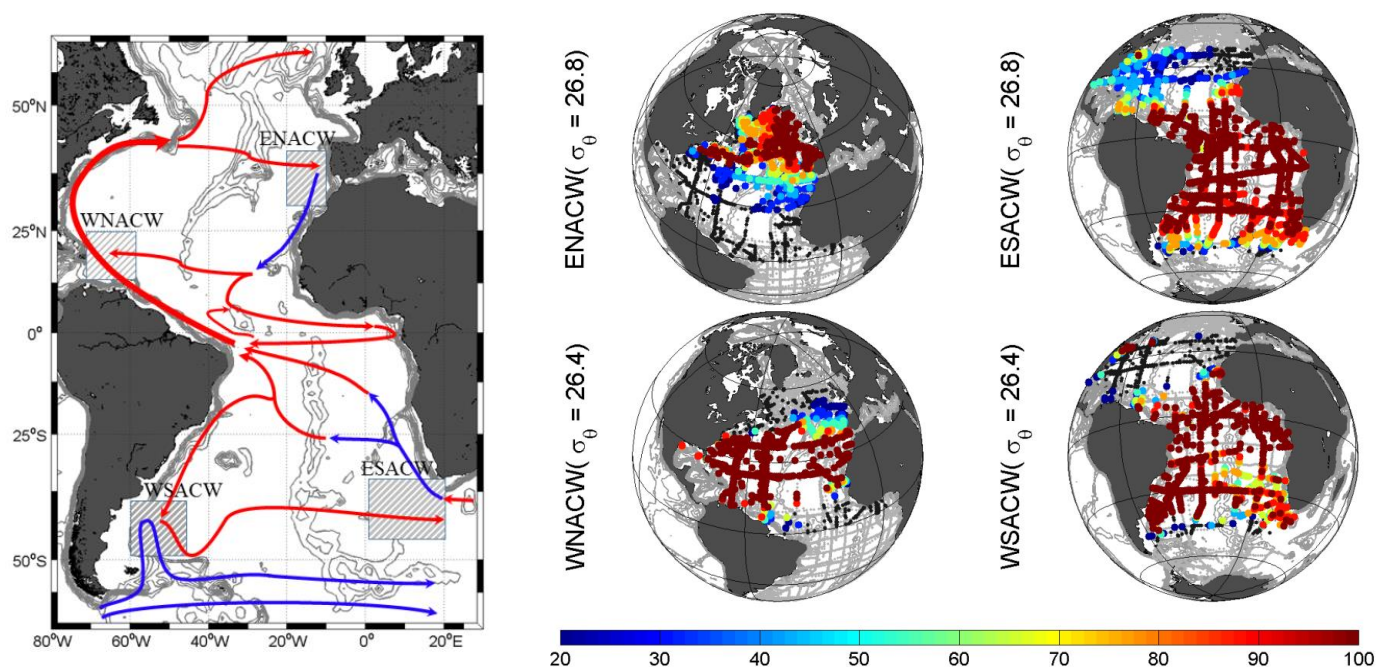


Fig. 3 Currents (left) and Water Masses (right) in the Upper Layer

Left: The arrows show the warm (red) and cold (blue) currents and rectangular shadow areas show the formation areas of water masses in the Upper Layer.

Right: Color dots show fractions (from 20% to 100%) of water masses in each station around core potential density (kg/m^3). Stations with fractions less than 20% are marked by black dots while gray dots show the GLODAPv2 stations without specified water mass.

549

550



551
 552

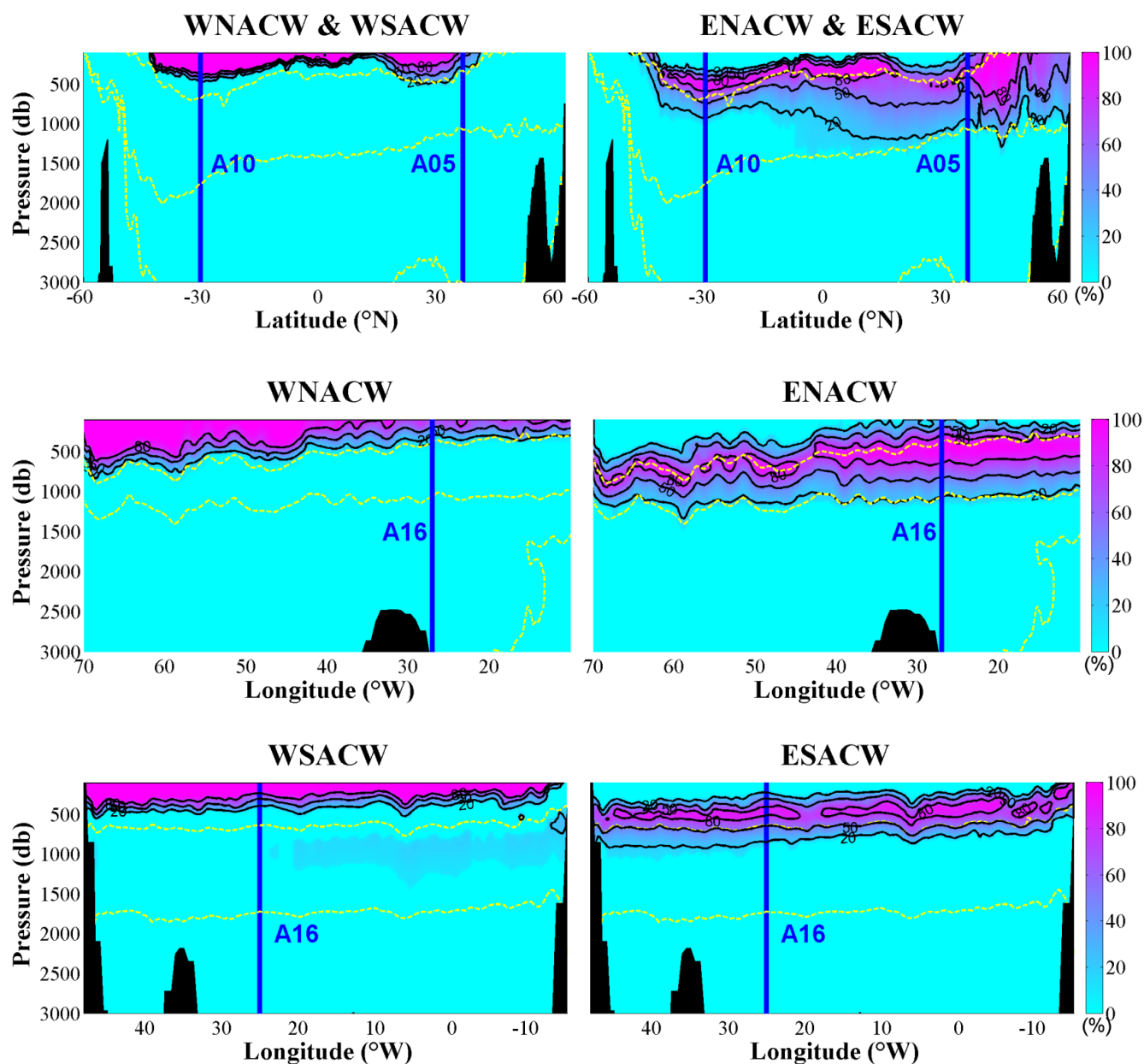


Fig. 4 Distribution of Central Water Masses based on A16 (upper), A05 (middle), A10 (lower) cruises within 3000m

Contour lines show fractions of 20% 50% and 80%, blue lines show cross section of other cruises, yellow dashed lines show the boundaries of vertical water columns layers (potential density at 27, 27.7 and 27.88 kg/m³)

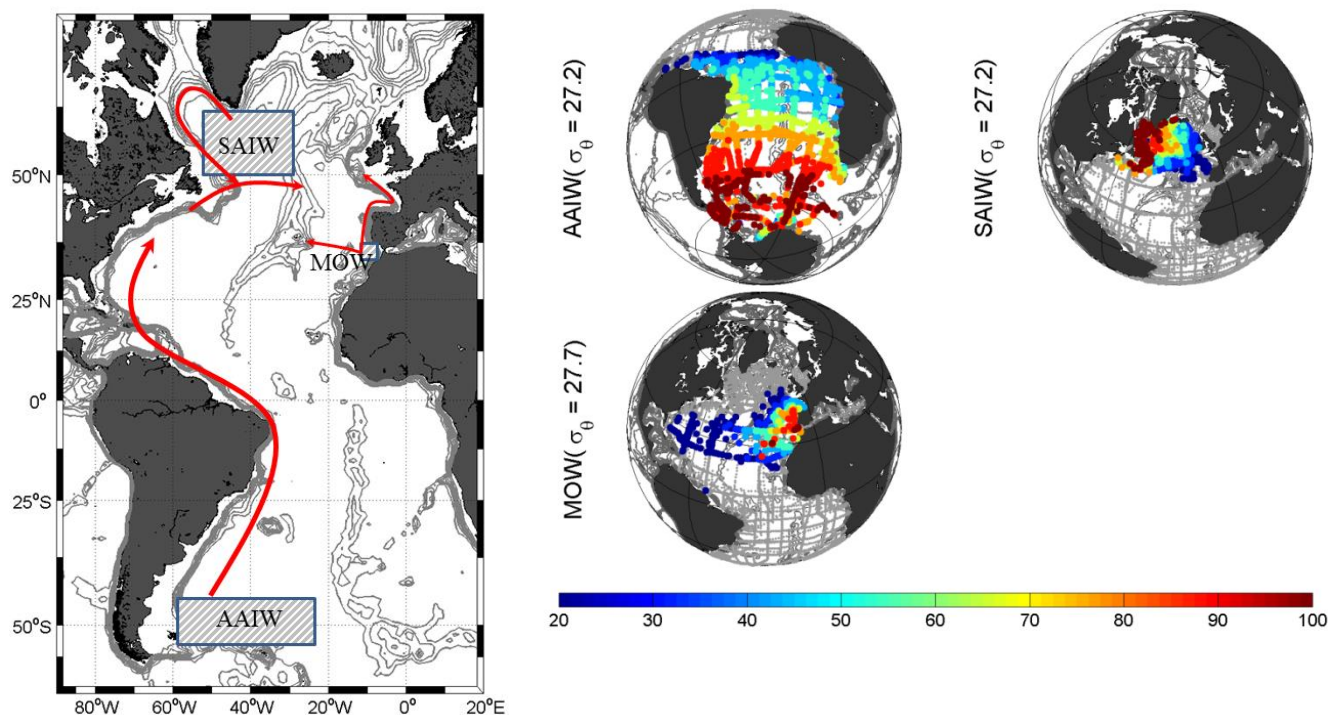


Fig.5 Currents (left) and Water Masses (right) in the Intermediate Layer

Left: The arrows show the currents and rectangular shadow areas show the formation areas of water masses in the Intermediate Layer.

Right: Color dots show fractions (from 20% to 100%) of water masses in each station around core potential density (kg/m^3). Stations with fractions less than 20% are marked by black dots while gray dots show the GLODAPv2 stations without specified water mass.

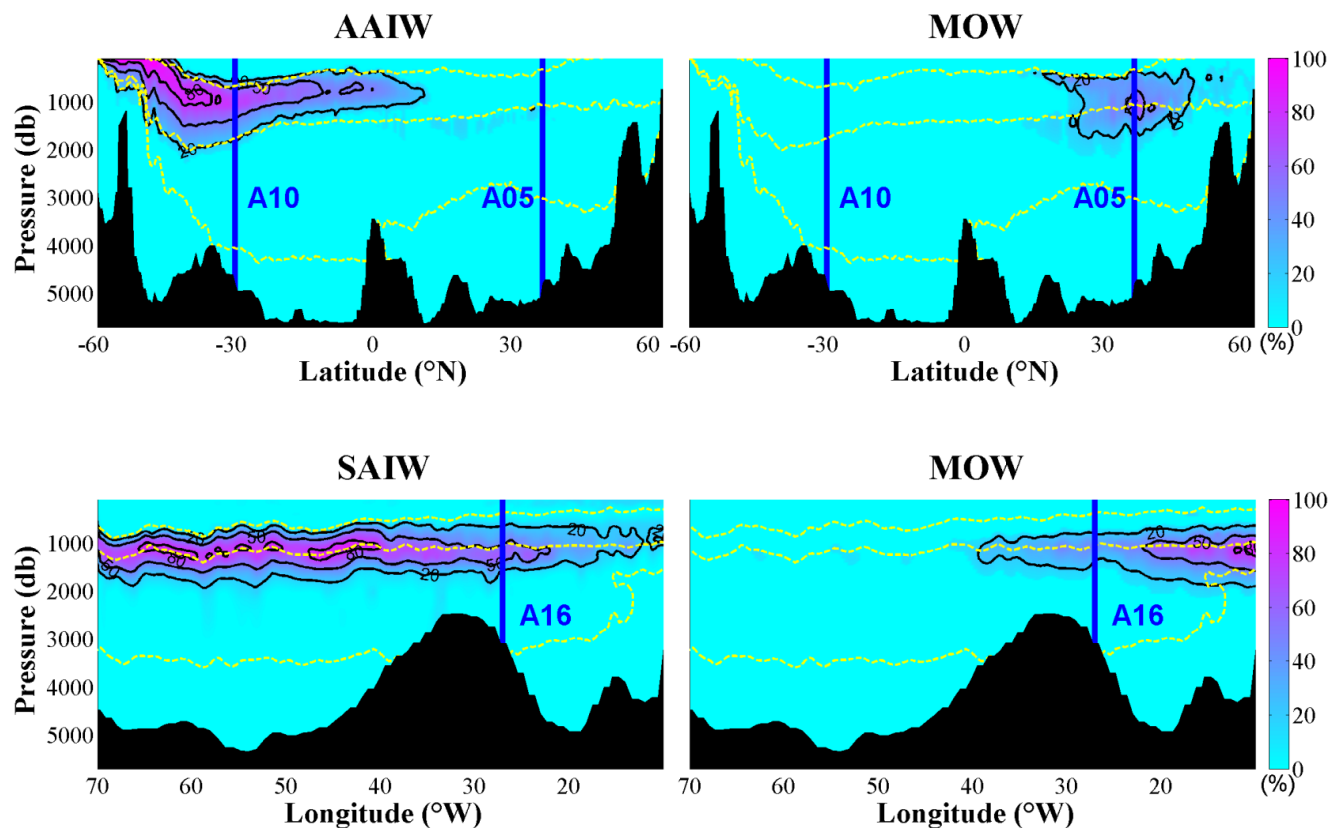


Fig. 6 Distribution of Water Masses in the Intermediate Layer based on A16 (upper) and A05 (lower) cruises

Contour lines show fractions of 20% 50% and 80%, blue lines show cross section of other cruises, yellow dashed lines show the boundaries of vertical water columns layers (potential density at 27, 27.7 and 27.88 kg/m³)

557

558

559

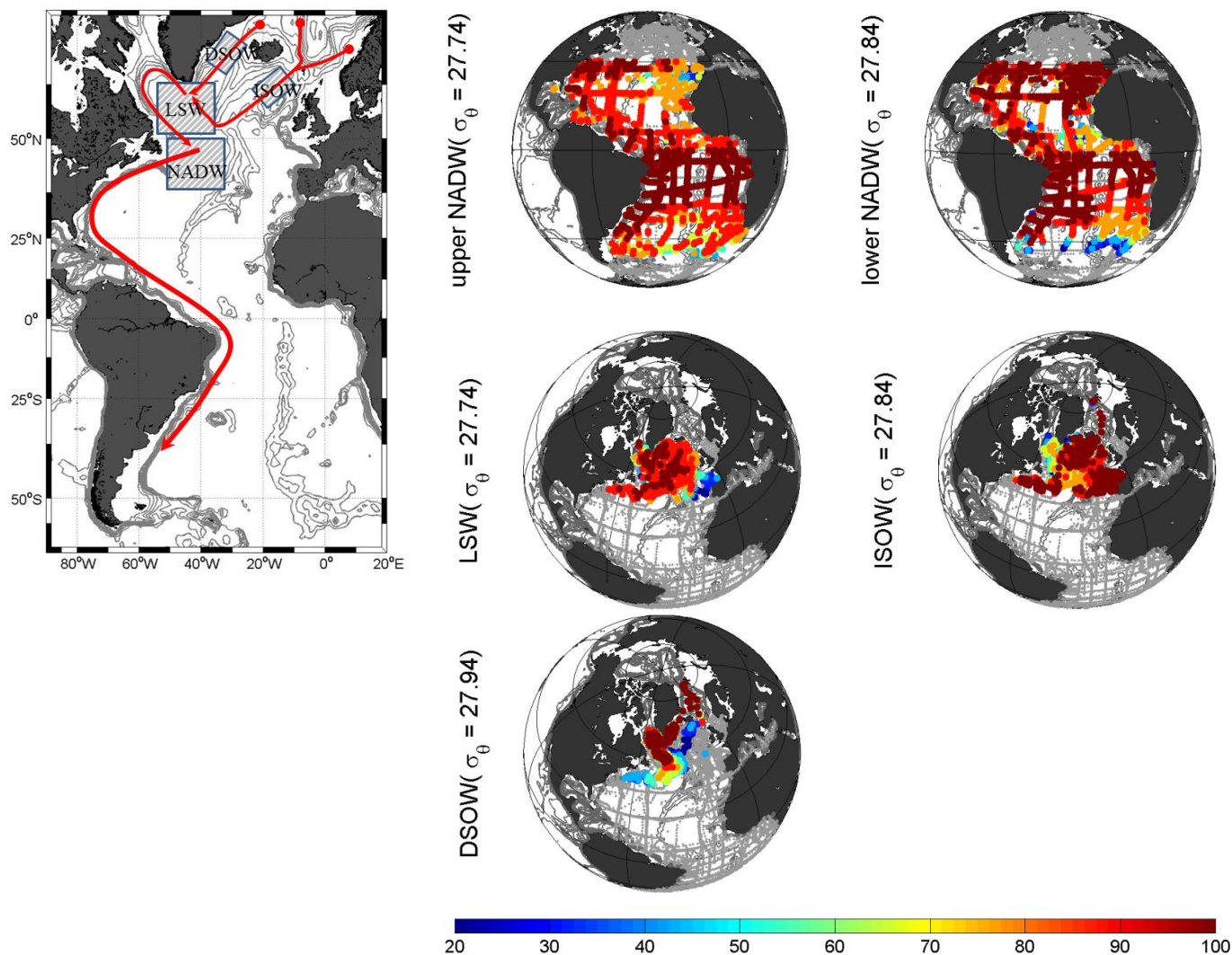


Fig.7 Currents (left) and Water Masses (right) in the Deep and Overflow Layer

Left: The arrows show the currents and rectangular shadow areas show the formation areas of water masses in the Deep and Overflow Layer.

Right: Color dots show fractions (from 20% to 100%) of water masses in each station around core potential density (kg/m^3). Stations with fractions less than 20% are marked by black dots while gray dots show the GLODAPv2 stations without specified water mass.



561

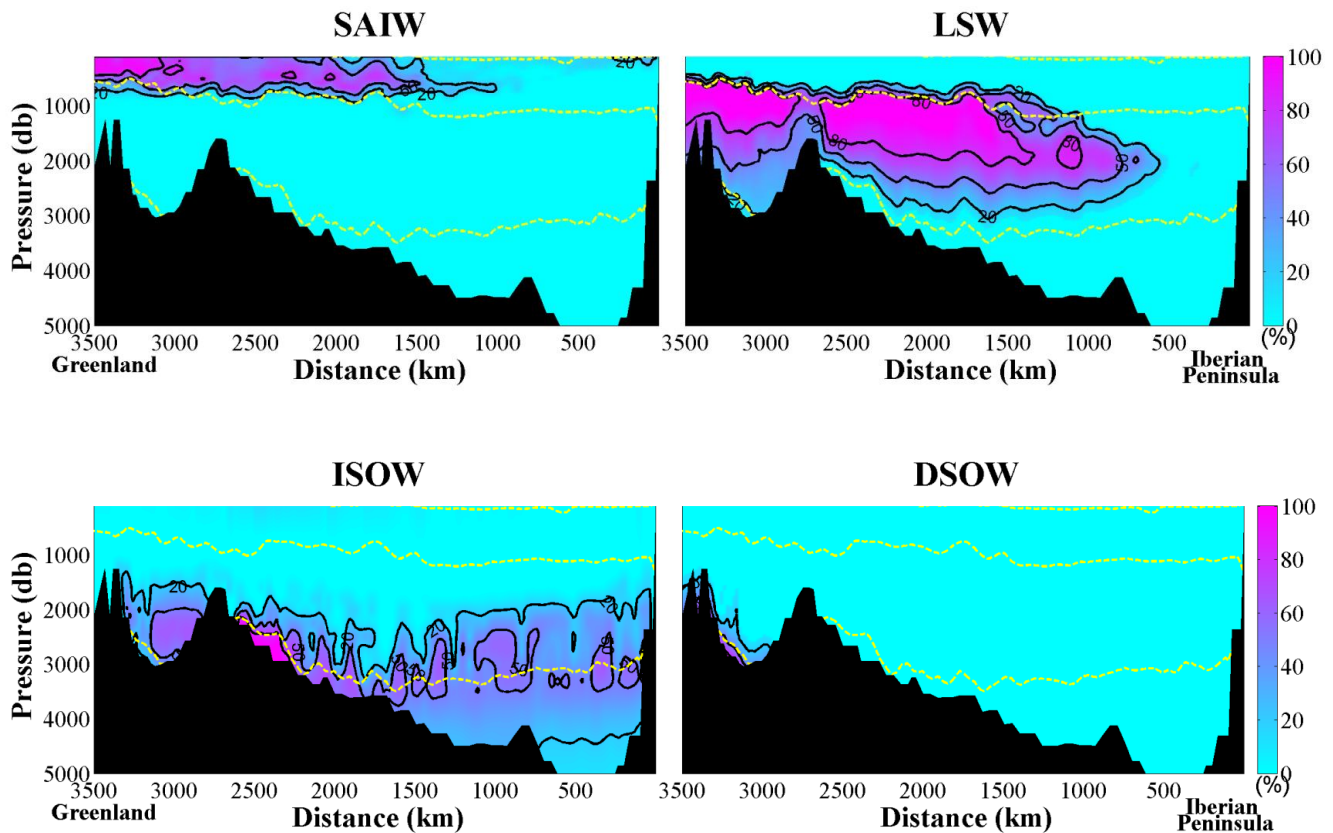


Fig. 8 Distribution of SAIW (upper left), LSW (upper right), ISOW (lower left) and DSOW (lower right) based on A25 cruise
Contour lines show fractions of 20% 50% and 80%, blue lines show cross section of other cruises, yellow dashed lines show the
boundaries of vertical water columns layers (potential density at 27, 27.7 and 27.88 kg/m³)

562

563

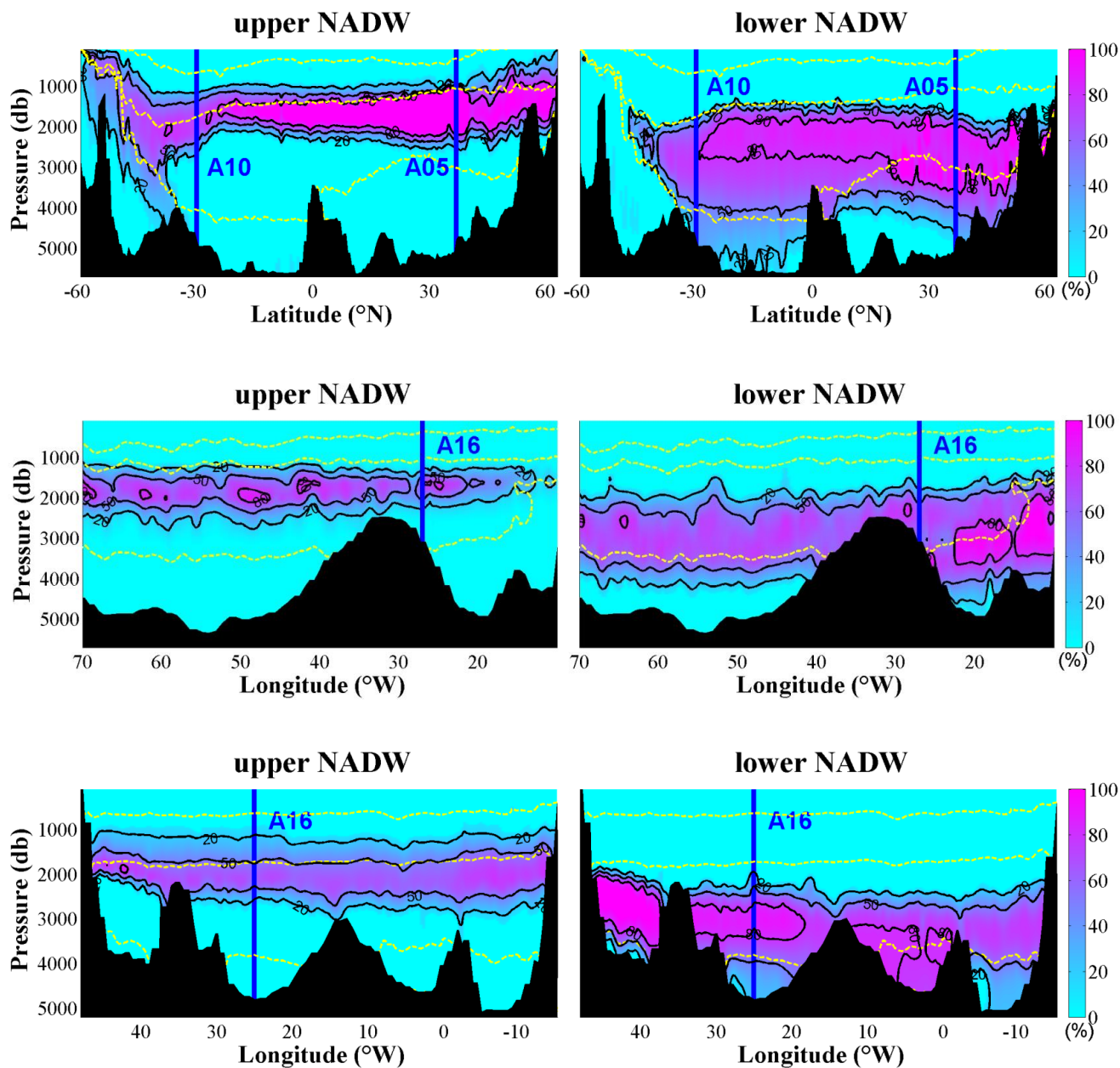


Fig. 9 Distribution of upper and lower NADW based on A16 (upper), A05 (middle) and A10 (lower) cruises

Contour lines show fractions of 20% 50% and 80%, blue lines show cross section of other cruises, yellow dashed lines show the boundaries of vertical water columns layers (potential density at 27, 27.7 and 27.88 kg/m³)

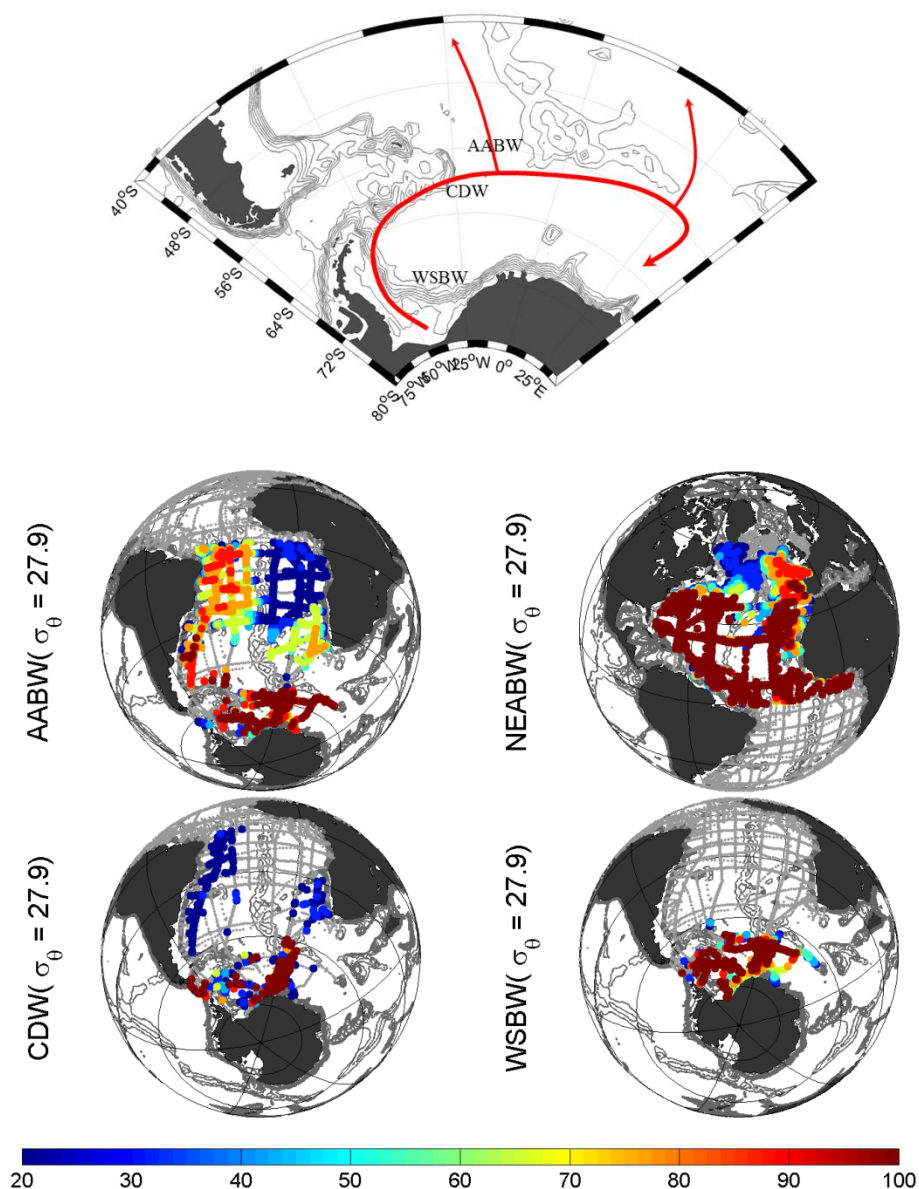


Fig.10 Currents (upper) and Water Masses (lower) in the Bottom Layer (AABW and NEABW) and the Southern Area (CDW and WSBW)

Upper: The arrows show the currents in the Southern Area.

Lower: Color dots show fractions (from 20% to 100%) of water masses in each station around core potential density (kg/m³). Stations with fractions less than 20% are marked by black dots while gray dots show the GLODAPv2 stations without specified water mass.



566

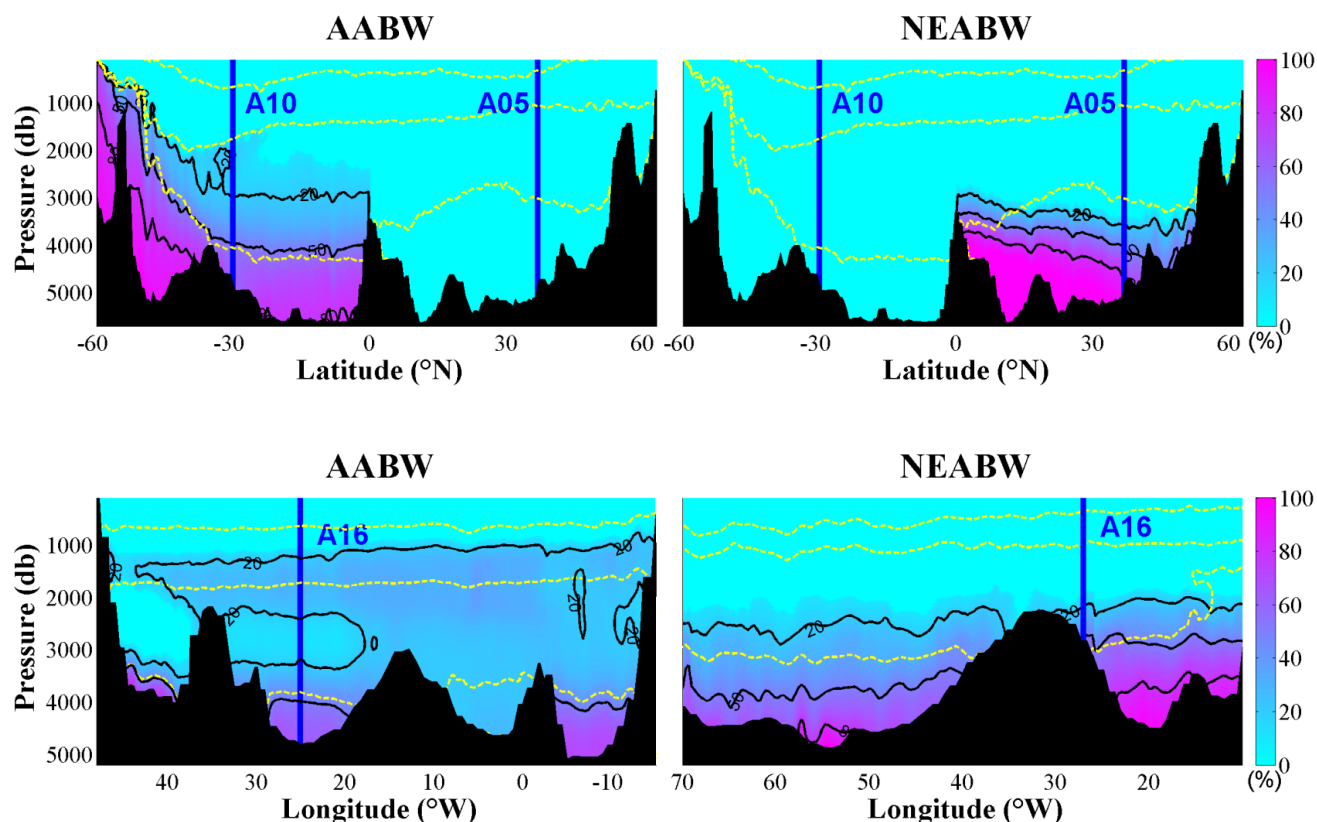


Fig. 11 Distribution of AABW and NEABW based on A16 (upper), A10 (lower left) and A05 (lower right) cruises

Contour lines show fractions of 20% 50% and 80%, blue lines show cross section of other cruises, yellow dashed lines show the boundaries of vertical water columns layers (potential density at 27, 27.7 and 27.88 kg/m³)

567

568

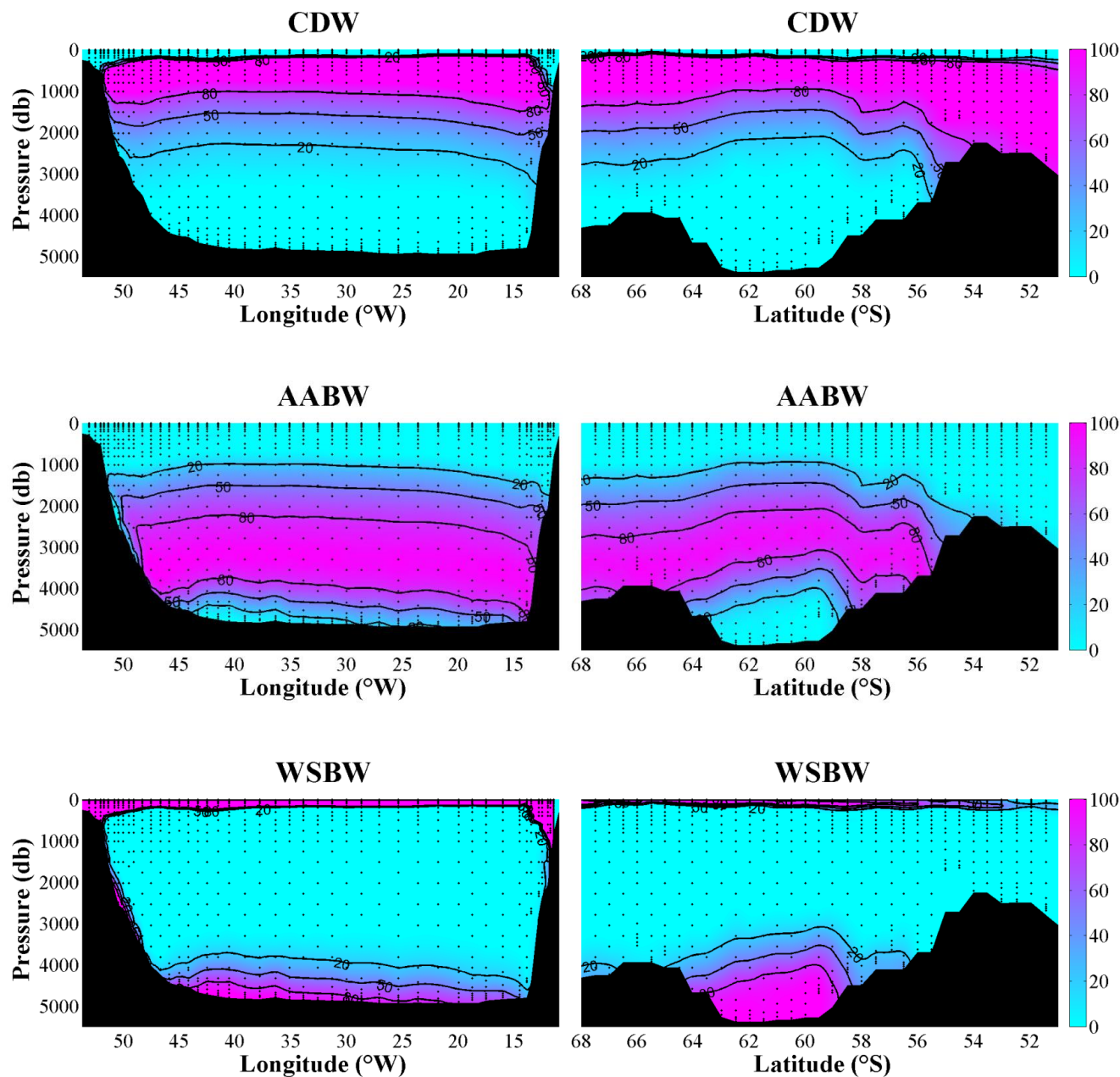


Fig. 12 Distribution of Southern Water Masses (CDW, AABW and WSBW) based on SR04 cruises

Left figures show the west (zonal) part and right figures show the east (meridional) part

Contour lines show fractions of 20% 50% and 80%, blue lines show cross section of other cruises



570

571

50 °S

Equator

40 °N

#13 AAIW AABW CDW WSBW $(\sigma_\theta = 27 \text{ kg/m}^3)$ $(\sigma_\theta = 27.7 \text{ kg/m}^3)$ $(\sigma_\theta = 27.88 \text{ kg/m}^3)$	#6 WSACW ESACW AAIW	#5 WSACW WNACW ESACW ENACW AAIW	#1 WNACW ENACW SAIW MOW
	#8 ESACW AAIW uNADW	#7 ENACW ESACW AAIW MOW uNADW	#2 ENACW SAIW MOW LSW
	#10 AAIW uNADW INADW CDW AABW	#9 AAIW MOW uNADW INADW NEABW	#3 SAIW LSW ISOW DSOW NEABW
	#12 INADW AABW	#11 INADW NEABW	#4 ISOW DSOW NEABW

572

50 °S

Equator

40 °N

573

Table 1 schematic of OMP runs in this study

574

575